Submillimetre negative differential conductivity at the cyclotron frequency in $Ga_{1-x}Al_xAs$ in strong $E \perp H$ fields

1997 J. Phys.: Condens. Matter 9 4659

(http://iopscience.iop.org/0953-8984/9/22/018)

J. Phys.: Condens. Matter **9** (1997) 4659–4667. Printed in the UK PII: S0953-8984(97)77413-7

Submillimetre negative differential conductivity at the cyclotron frequency in $Ga_{1-x}Al_xAs$ in strong $E \perp H$ fields

G E Dzamukashvili, Z S Kachlishvili and N K Metreveli
Tbilisi State University, Chavchavadze st. 3, Tbilist, 380028, Republic of Georgia

Received 27 August 1996, in final form 9 January 1997

Abstract. In this paper it is shown theoretically that under certain conditions a cyclotron resonance maser based on $Ga_{1-x}Al_xAs$-type materials can be fabricated. Strong crossed electric and magnetic fields ($\boldsymbol{E} \perp \boldsymbol{H}$), in which electrons in the central (Γ) conduction band valley move dynamically (ballistically) up to the energy of the onset of intervalley scattering ε_0, are considered. The working temperatures of these masers could be increased to 80 K.

The investigations have been carried out for the solid-solution composition with $0 < x < 0.39$ ($\varepsilon_0 = (2\text{–}17)\hbar\omega^*$, where $\hbar\omega^*$ is the intervalley phonon energy). The values of the fields E and H varied within the ranges $E = 5\text{–}20$ kV cm^{-1}, and $H = 5\text{–}60$ kOe. This caused a smooth change in the transit conditions in the passive region ($\varepsilon < \varepsilon_0$) which allows one to obtain the desired frequency dependence of the differential conductivity $\sigma(\omega)$. The investigations showed that under these conditions the earlier unexplained interesting peculiarities of the hot-electron system appear.

In particular, it is shown that there is a resonance in the $\sigma(\omega)$ dependence near the cyclotron frequency $\omega \approx \omega_c$. At the same time the dynamic negative differential conductivity (DNDC) appears. In this case the static differential conductivity is positive. This is very important since realization of the static positive differential conductivity with DNDC remaining unchanged has so far been problematic for materials of GaAs type. The DNDC frequency is in the submillimetre range and can be changed smoothly with change in E and H

1. Introduction

A problem of great importance in solid-state electronics is the assimilation of the submillimetre (far-infrared) range of the electromagnetic spectrum. At the end of the 1980s, investigations of nearly 30 year duration were completed by the creation of masers based on p-Ge, operating in the above-mentioned spectral range. However, they have not found wide use in techniques, principally because of the restriction on the operating temperature ($T = 4$ K). So the search for ways to solve the above-mentioned problem is still in progress.

In recent years [1–3] the possibility of creating generators covering the frequency range up to 5000 GHz on the basis of quantum superlattices has been shown. Despite the fact that these investigations are very hopeful, the search for ways to solve the problem traditionally (using volume effects) has also carried on [4, 5]. In fact, as is shown in [4] when substituting Faraday's configuration for Voight's configuration, on the one hand, the maser's radiation intensity increases considerably and, on the other hand, generation is observed near liquid-nitrogen temperature. The latter circumstance is of particular importance. It has been shown in [5] that, when ballistic intervalley transfer of electrons takes place in $Ga_{1-x}Al_xAs$ in strong transverse electric and magnetic fields, under certain conditions a submillimetre dynamic negative differential conductivity (DNDC) arises. In the present work the theory developed in [5] is extended to the case when part of the phase trajectories is closed. Additional factors affecting the DNDC rise are also revealed and optimal values of external fields and solid-solution composition favourable to DNDC rise in the terahertz frequency range are recommended.

2. Approximations used in the work and scheme of the intervalley transitions

The crystal temperature T must satisfy the condition

$$k_0 T \ll \hbar\omega^*. \tag{1}$$

At this temperature, intervalley transitions (IVTs) can be realized only with spontaneous emission of non-polar optical phonons with an energy $\hbar\omega^* = 0.8\hbar\omega_0$ (ω_0 is the frequency of the polar optical phonon). In this case, IVTs begin only when electrons reach the energy $\varepsilon_0 = \Delta\varepsilon + \hbar\omega^*$, where $\Delta\varepsilon$ is the energy gap between the Γ and X valleys (figure 1(a)).

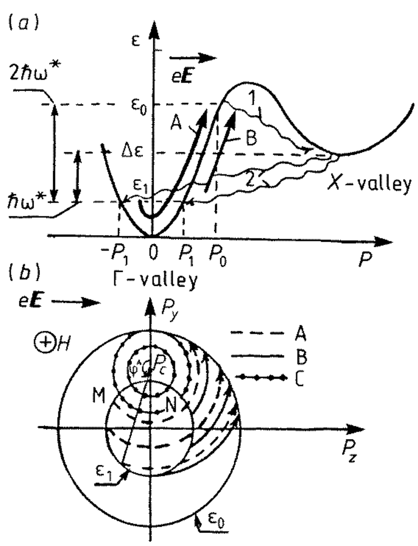

Figure 1. (*a*) A schematic diagram of IVTs and (*b*) their distribution in the momentum space of the Γ valley in the two-valley model of the conduction band of $Ga_{1-x}Al_xAs$ semiconductor. Γ is the 'light' valley, X is the 'heavy' valley, 1 is the Γ → X transition, 2 is the X → Γ transitions, and A and B are the free (ballistic) motions of A and B electrons. On the C trajectories, electrons are closed in the magnetic 'trap'. $P_c = c_0 m_\Gamma^* E_0/H$. The analytical expression for the angle φ^A is given in section 3.

The constant electric field $\boldsymbol{E}_0$ is such that the condition of dynamic heating in the Γ valley is fulfilled:

$$\tau_E = \nu_E^{-1} = \frac{P_0}{eE_0} < \tau_{PO} = \nu_{PO}^{-1} \tag{2}$$

where τ_{PO} is the specific time of electron scattering by polar optical phonons inside the Γ valley, τ_E is the transit time of electrons up to the energy ε_0, and $P_0 = \sqrt{2m_\Gamma^*\varepsilon_0}$ (where m_Γ^* is the effective mass of the electrons in the Γ valley).

The distribution function f_x in X valleys is considered to be in equilibrium with the lattice temperature [6].

It is easy to verify that at temperatures satisfying condition (1) the Dirac δ function is a good approximation of the distribution function f_x. Therefore, the 'arrival' band width in the Γ valley will be negligibly small, and in momentum space it is depicted as a spherical surface $\varepsilon_1 = \Delta\varepsilon - \hbar\omega^* =$ constant where acceleration of electrons occurs (figure 1(b)).

When electrons acquire the energy ε_0, a strong inelastic scattering with a specific frequency τ_0^{-1} comes into play. Since τ_0 is a small parameter (see, e.g., [7]), the energy region $\varepsilon > \varepsilon_0$ (active region or exit region) will be narrow, and its contribution to the conductivity will be neglected. The validity of this assumption is discussed in detail in section 5.

From the above reasoning, with $e\boldsymbol{E}_0 \uparrow\uparrow \boldsymbol{Z}_0$ and $\boldsymbol{H} \uparrow\uparrow \boldsymbol{X}_0$, we have the dynamic IVT situation shown in figure 1(a). The diagram shows explicitly two groups of electrons (A and B) which begin to move in the momentum space from different semispheres: $\varepsilon_1 =$ constant, $P_z < 0$; $\varepsilon_1 =$ constant, $P_z > 0$.

Electrons rotate in the $P_x =$ constant plane. The centres of the phase trajectories lie on the $(P_x, P_c, 0)$ segment, where $-P_1 < P_x < P_1$ and $P_1 = \sqrt{2m_\Gamma^*\varepsilon_1}$. Therefore, at a fixed $\Delta\varepsilon$ the electron distribution in the momentum space is unambiguously described by the P_c-value which is determined by the E_0/H ratio: $P_c = c_0 m_\Gamma^* E_0/H$.

Let P_1' and P_0' denote the radii of the circles formed by intersection of the spherical surfaces $\varepsilon_1 =$ constant and $\varepsilon_0 =$ constant and the plane $P_x =$ constant: $P_1' = \sqrt{P_1^2 - P_x^2}$; $P_0' = \sqrt{P_0^2 - P_x^2}$. Electrons that start to move from the narrow band (i.e. situated along the circle with the radius P_1') and cross the circle with the radius P_0' pass into the X valley. Hence, the phase trajectories of these electrons are open. If at a certain $(P_x)_1$ condition $P_c \geqslant (P_0' + P_1')/2$ is fulfilled, phase trajectories will be open for all P_x, whose absolute value exceeds $(P_x)_1$. From the above it might be assumed that, if in the $P_x = 0$ plane all trajectories are open, i.e. if

$$P_c > \frac{P_0 + P_1}{2} \equiv P_c^* \tag{3}$$

all trajectories will also be open throughout the whole phase space. Condition (3), in turn, imposes a restriction on the values of electric and magnetic fields, which allows one to determine the maximum value H^* of the magnetic field with $E_0 =$ constant, and the minimum value (E_0^*) of the electric field with $H =$ constant.

When P_c lies in the range

$$P_{c1} \equiv \frac{P_0 - P_1}{2} < P_c < P_c^* \tag{4}$$

closed trajectories of 'C' type appear (figure 1(*b*)). The arrival of electrons on these trajectories (as well as on the open trajectories) occurs because of X $\rightarrow$ Γ transitions. In this case, trajectories of A, B and C type coexist in the phase space of the Γ valley. In this case it is evident that high-frequency characteristics of electrons moving along the open and closed trajectories should be studied independently. Unlike the electrons in groups A and B that warm up ballistically, for electrons in group C the intravalley scattering by phonons should be taken into account, since the electrons can leave the closed trajectories only because of such scattering.

3. The kinetic equation and the expression for the differential conductivity

The investigation was carried out using the distribution function obtained from the solution of the Boltzmann kinetic equation in the variable field $\boldsymbol{E}_\sim$ with a small amplitude brought into the system as a small perturbation and directed along $\boldsymbol{E}_0$: $\boldsymbol{E} = \boldsymbol{E}_0 + \boldsymbol{E}_\sim$, $\mathbf{E}_\sim = \boldsymbol{E}^0_\sim \exp(\mathrm{i}\omega t)$, $E^0_\sim \ll E_0$ and $\boldsymbol{E}_\sim \parallel \boldsymbol{E}_0$. In this case a small alternating part $f_\sim$ is added to the distribution function which exists in constant fields $\boldsymbol{E}_0 \parallel \boldsymbol{H}$: $f = f_0 + f_\sim$, $f_\sim = f^0_\sim \exp(\mathrm{i}\omega t)$, and $f^0_\sim \ll f_0$. With allowance for the above-mentioned approximations we obtain a linearized equation for $f^0_\sim$:

$$\mathrm{i}\omega f^0_\sim + \omega_c \frac{\partial f^0_\sim}{\partial \varphi} = -eE^0_\sim \frac{\partial f_0}{\partial P_z} - \frac{f^0_\sim}{\tau_{PO}} \qquad \varepsilon < \varepsilon_0. \tag{5}$$

For f_0 and the condition of conservation of the total number of electrons in the conduction band we have

$$\omega_c \frac{\partial f_0}{\partial \varphi} = \frac{N_x \nu_1}{2\pi P_1} \delta(P^2 - P_1^2) - \frac{f_0}{\tau_{PO}} \qquad \varepsilon < \varepsilon_0 \tag{6}$$

$$\int f_0 \, \mathrm{d}^3 P + N_x = N_0 = \text{constant} \tag{7}$$

where N_0 and N_x are the total electron concentration in the conduction band and the electron concentration in X valleys, respectively. $\nu_1 = \mathcal{D}^2_{\Gamma x} (m^*_\Gamma)^{3/2} \sqrt{\varepsilon_1} / \sqrt{2}\pi \hbar^3 \rho \omega^*$ is the characteristic frequency of the X $\rightarrow$ Γ valley transitions, $\mathcal{D}_{\Gamma x}$ is the intervalley deformation potential field, ρ is the sample density and $\tan\varphi = P_z/(P_c - P_y)$. The factor before the δ function is associated with the normalization condition (7). The second summands on the right-hand sides of equations (5) and (6) appear only on closed trajectories.

The differential conductivity is given only in the form of a triple integral without indicating an explicit form of the distribution function and integration limits (owing to their complexity):

$$\sigma_{oup}(\omega) = \sigma^A_{oup}(\omega) + \sigma^B_{oup}(\omega). \tag{8}$$

Here σ^A_{oup} and σ^B_{oup} are the conductivities of electrons that move along the A and B trajectories, respectively:

$$\sigma^{A,B}_{oup}(\omega) = \sigma_0 \frac{\beta}{4\pi\alpha} \frac{1}{1 - \Omega_c^2} \iiint_{\Sigma^{A,B}_{oup}} \frac{\sin\varphi}{|\sin\varphi^A|} \{(1 + \Omega_c^2)\cos\varphi^A \cos\Omega_c(\varphi - \varphi^{A,B}) - 2\Omega_c \sin\varphi^{A,B} \sin\Omega_c(\varphi - \varphi^{A,B}) - 2\cos\varphi\} \, \mathrm{d}x \, \mathrm{d}r \, \mathrm{d}\varphi$$

where $\sigma_0 = e^2 N_x \nu_1 / m^*_\Gamma \nu_E^2$, $\varphi^A = \cos^{-1}[(P_1^2 - P_x^2 - P_r^2 - P_c^2)/2P_c P_r]$, $\varphi^B = 2\pi - \varphi^A$ and $P_r = [P_z^2 + (P_y - P_c)^2]^{1/2}$. The physical meaning of the angle φ^A is explained in figure 1(*b*). $\beta \equiv P_c/P_0 = \nu_E/\omega_c$, $\alpha \equiv \sqrt{\varepsilon_1/\varepsilon_0} = P_1/P_0$, $\Omega_c \equiv \omega/\omega_c$, $x = P_x/P_0$ and $r = P_r/P_0$.

The integration regions Σ^A_{oup} and Σ^B_{oup} are created by combination of open trajectories of A and B electrons, respectively.

The solid-state composition varied within the wide range $0 < x < 0.39$ and, accordingly, $\Delta\varepsilon$ varied within the range (1–16)$\hbar\omega^*$. The applied electric and magnetic fields varied within the ranges $E_0 = 5$–20 kV cm^{-1} and $H = 5$–60 kOe. The differential conductivities of different groups of electrons were calculated separately for each value of $\Delta\varepsilon$.

To obtain the total differential conductivity σ in the Γ valley, one should, naturally, add up conductivities of all types of electrons existing in this valley, i.e. a sum of separate parts of the differential conductivity should be taken:

$$\sigma = \sigma^A + \sigma^B \qquad \sigma^A = \sigma^A_{oup} + \sigma^A_{cl} \qquad \sigma^B = \sigma^B_{oup} + \sigma^B_{cl}.$$

Here σ^A_{cl} and σ^B_{cl} are the conductivities of electrons that move along the C trajectories. The role of these electrons in the total conductivity will be discussed in section 4.

4. Selection of parameters for formation of the dynamic negative differential conductivity with the highest frequency

4.1. The role of electrons moving along closed cyclotron trajectories

It is well known that, when the volume of the region of dynamic motion of electrons is $\hbar\omega_0$, electron redistribution between open and closed trajectories takes place only because of intravalley phonon scattering [8]. It is also known that electrons which have accumulated in the magnetic trap (created by combination of closed cyclotron trajectories inside the passive region $\varepsilon < \hbar\omega_0$) do not contribute to transport phenomena along the $\boldsymbol{E}_0$ field.

In our case the situation is quite different. Electron transitions from C to open trajectories result from inelastic scattering by optical phonons, but electron transitions from open to closed trajectories take place only through their transitions in the X valley. Therefore, in the spindle-like region (which is created by a combination of C-type trajectories) there is an area where a larger number of electrons arrive. In the YOZ plane this area is shown by the arc MN (figure 1(b)). This circumstance distinguishes radically the case of dynamic electron motion inside a single valley within the energy range $0 < \varepsilon < \varepsilon_0 = \hbar\omega_0$ from that of dynamic IVTs, when ε_0 is several times larger than $\hbar\omega_0$ (in the latter case the spindle-like region is energetically much larger than the energy $\hbar\omega_0$). This difference manifests itself in the fact that the distribution functions f_c^A and f_c^B on the C trajectories are not symmetrical along $\boldsymbol{E}_0(\partial f_c^A/\partial P_z \neq 0; \partial f_c^B/\partial P_z \neq 0)$. Therefore the differential conductivities of these electrons will differ from zero.

4.2. Conditions imposed on electric and magnetic fields

Let us consider factors hindering and favouring the appearance of DNDC. The resonance-type DNDC investigated at $P_c > P_c^*$ in [5] continues to increase with further increase in the magnetic field (when P_c becomes smaller but closer to P_c^*). This increase in DNDC is due to enhancement of transit effects with increasing cyclotron frequency. This enhancement occurs against the background of a slight decrease in the number of electrons on the open trajectories.

A further increase in H decreases the volumes Σ_{oup}^A and Σ_{oup}^B. This results in decreases in the resonance peak in the $\sigma_{oup}(\omega)$ dependence and the resonance line half-width, but a relatively large number of electrons with a positive but low differential conductivity are accumulated on the closed trajectories. The two factors hinder the condition for DNDC appearance. Enhancement of 'transit' resonance is the only factor contributing to the appearance of the DNDC with increasing H. Despite the above-mentioned difficulties an increase in the H field is still important in the search for a high ω_c in the vicinity of which DNDC appears.

It has been established that for each $\Delta\varepsilon$ there is a minimum value $(P_c)_{min}$ such that at $P_c < (P_c)_{min}$ the existence of DNDS is doubtful. The condition $P_c > (P_c)_{min}$ imposes either an upper limit on an allowed value of the magnetic field at a given E_0, or a lower limit on E_0 at a given H. Imposition of an upper limit on H restricts the cyclotron frequency. If H_c denotes the magnetic field which favours the entry of ω_c into the submillimetre region, the region of allowed values of H at a given E_0 is determined by the inequalities

$$H_c < H < \frac{c_0 m_\Gamma^* E_0}{(P_c)_{min}}. \tag{9}$$

At a fixed H condition, (9) imposes the condition on the electric field which must be higher than $E_{min} = (P_c)_{min} H_c / c_0 m_\Gamma^*$ but the field E_0 must be such that the ballistics condition (2) could be fulfilled. It is also evident that the particular values of E_{min} and the parameters of condition (2) depend on $\Delta\varepsilon$.

The value of H can be changed both at a fixed P_c (when the electric field varies proportionally to H) and with a simultaneous change in P_c (at a fixed E_0). It should be noted that the variations in H in these two cases have different influences on the degree of electron redistribution inside the Γ valley and give, accordingly, different quantitative effects in the DNDC formation. In the first case the ratio ω_c/ν_{PO} changes when the volume Σ_{cl} remains unchanged (Σ_{cl} is created by the combination of closed trajectories). In the second case an increase in the magnetic field results in increases in Σ_{cl} and ω_c/ν_{PO}. In the second case the increase in the magnetic field should exert a stronger influence on the $\sigma(\omega)$ dependence than in the first case. It should be mentioned that the Σ_{cl} region with the same ω_c/ν_P can be changed only by changing E_0 with the same H.

It is not difficult to obtain numerical values of parameters and threshold fields at all $\Delta\varepsilon$ under consideration, since the analytical dependences of the band-structure parameters on x for $Ga_{1-x}Al_xAs$ have been extensively investigated and are well known. These results are summarized in [9].

5. Results and discussion

When $\Delta\varepsilon \gg \hbar\omega^*$ a decrease in P_c (an increase in H) gradually suppresses the DNDC created in the strong electric field by B-group electrons [7]. This DNDC is fully associated with electron transit effects in the Γ valley (transit DNDC). At $\Delta\varepsilon = 16\hbar\omega^*$ (GaAs), the transit DNDC completely disappears when $P_c = 0.3P_0$, but with this P_c ($E = 20$ kV cm^{-1}; $H = 42$ kOe) a resonance DNDC appears in the vicinity of ω_c within the frequency range 1700 GHz $< \nu <$ 2000 GHz, which is deep in the submillimetre region. For $P_c > 0.3P_0$ the resonance frequency decreases and the conditions for the resonance DNDC are hindered. This deterioration is caused essentially by the wide scatter in the frequency of A-group transit electrons that give a positive differential conductivity with a higher absolute value than a negative differential conductivity of B electrons. For the above-mentioned $\Delta\varepsilon$, realization of the resonance DNDC over a wide range of E_0 and H does not occur.

The suppression of the transit DNDC of B electrons by the magnetic field and the influence of this field on the total differential conductivity is more effective at smaller $\Delta\varepsilon$ (although at $\Delta\varepsilon < 4\hbar\omega^*$ the transit DNDC in the electric field is absent owing to the scatter of transit frequencies in the various groups of electrons). The influence of the magnetic field on the differential conductivity at a fixed $\Delta\varepsilon$ can be seen by comparison of the curves in figures 2(a) and 2(b).

The effect of a simultaneous change in E_0 and H fields at a fixed P_c is illustrated in figures 2(b) and 2(c). At all $\Delta\varepsilon$-values the change in P_c changes the dependence $\sigma(\omega)$ qualitatively, while the change in E_0 and H fields at a fixed P_c causes only a quantitative change. This influence of the field on the differential conductivity becomes stronger, as P_c decreases.

The parameter ν_{PO} in our calculations does not depend on the energy. We have thoroughly investigated the influence of the ν_{PO}-value on the total differential conductivity and established that this influence increases with decreasing $\Delta\varepsilon$. However, as is seen from a comparison of the curves in figures 3(a) and 3(b), even at the smallest value of $\Delta\varepsilon = 1.7\hbar\omega^*$ ($Ga_{0.63}Al_{0.37}As$) a twofold change in ν_{PO} does not significantly affect the $\sigma(\omega)$ dependence. This influence will be less pronounced at high $\Delta\varepsilon$.

Detailed investigation of the static negative differential conductivity (SNDC) has shown that it decreases with increasing magnetic field, and in the case of small $\Delta\varepsilon(\Delta\varepsilon < 3\hbar\omega^*)$

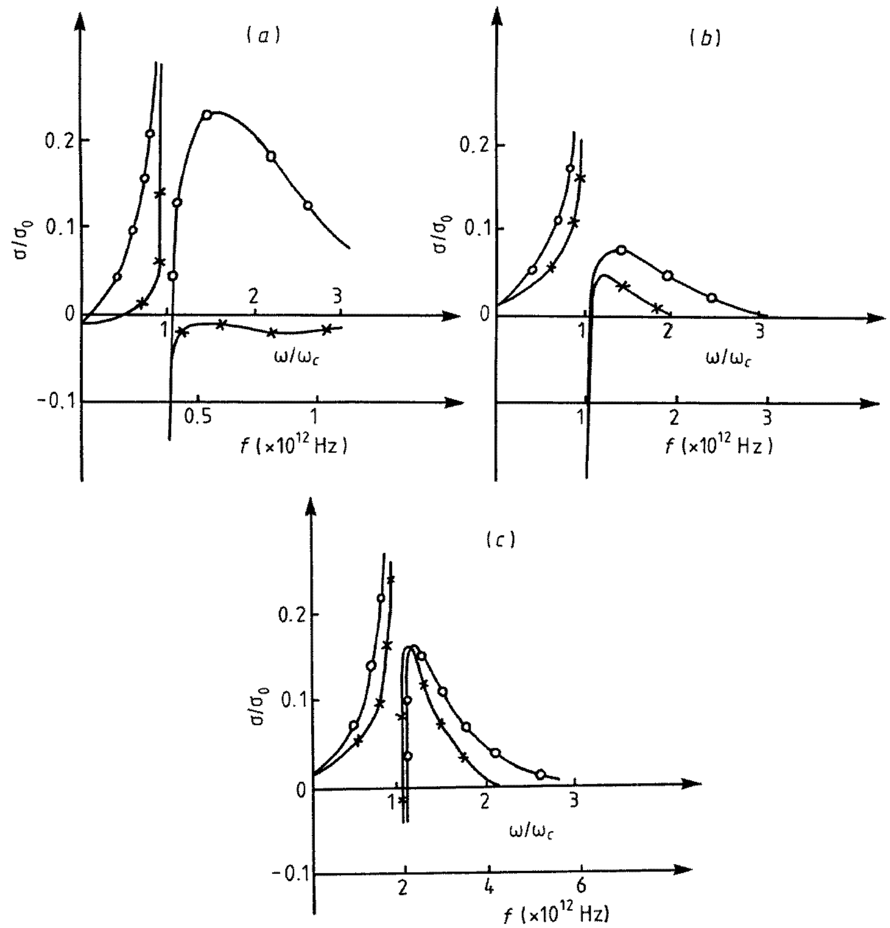

Figure 2. Differential conductivity at $\Delta\varepsilon = 10\hbar\omega^*$ ($Ga_{0.84}A_{0.16}As$) for (*a*) $P_c = 0.8P_0$, $E_0 = 10$ kV cm^{-1}, $H = 10.5$ kOe, $\omega_c = 2.3 \times 10^{12}$ s^{-1}, $\tau_{PO} = 1 \times 10^{-12}$ s, (*b*) $P_c = 0.3P_0$, $E_0 = 10$ kV cm^{-1}, $H = 28$ kOe, $\omega_c = 6.1 \times 10^{12}$ s^{-1}, $\tau_{PO} = 1 \times 10^{-12}$ s and (*c*) $P_c = 0.3P_0$, $E_0 = 20$ kV cm^{-1}, $H = 56$ kOe, $\omega_c = 12.2 \times 10^{12}$ s^{-1}, $\tau_{PO} = 10^{-12}$ s; ○ , $\sigma^A = \sigma^A_{oup} + \sigma^A_{cl}$; ×, $\sigma^B = \sigma^B_{oup} + \sigma^B_{cl}$.

it becomes positive even for fields close to H^*. In a strong magnetic field ($H > H^*$) the SNDC decreases substantially only for average values of $\Delta\varepsilon$: $\Delta\varepsilon = (3\text{–}8)\hbar\omega^*$. The result obtained is very important, because under these conditions we can remove low-frequency oscillations caused by the static differential conductivity.

The results of the investigations are of a common character and can be used for other materials of $Ga_{1-x}Al_xAs$ type. As for the $Ga_{1-x}Al_xAs$ parameters used in our estimations, the following should be mentioned: the constant $\mathcal{D}_{\Gamma x}$ of the relationship between Γ and the upper bands is not well established for $Ga_{1-x}Al_xAs$ and serves as a fitting parameter in the calculations [9]. The band width of $\varepsilon > \varepsilon_0$ depends strongly on its value. Penetration of electrons into this region increases their heating time and makes a positive contribution to the differential conductivity. On the other hand, such penetration blurs the clear picture depicted in figure 1(b). The frequency ν_0 of the $\Gamma \rightarrow X$ transition is very important in

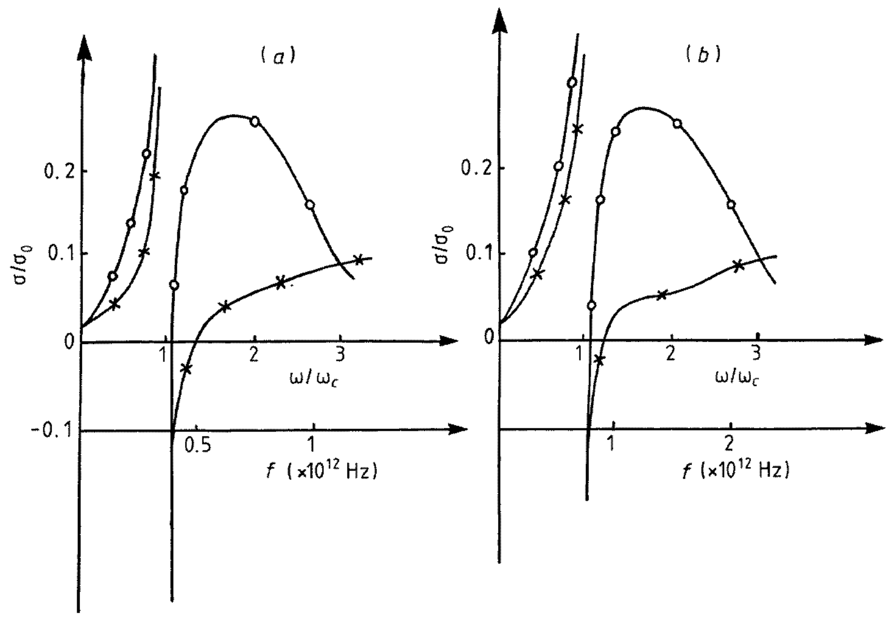

Figure 3. Differential conductivity at $\Delta\varepsilon = 1.7\hbar\omega^*$ ($Ga_{0.63}Al_{0.37}As$) for (*a*) $P_c = 0.7P_0$, $E_0 = 5$ kV cm^{-1}, $H = 13$ kOe, $\omega_c = 2.3 \times 10^{12}$ s^{-1}, $\tau_{PO} = 1 \times 10^{-12}$ s and (*b*) $P_c = 0.7P_0$, $E_0 = 5$ kV cm^{-1}, $H = 13$ kOe, $\omega_c = 2.3 \times 10^{12}$ s^{-1}, $\tau_{PO} = 2 \times 10^{-12}$ s: the symbols are as in figure 2.

establishing the width of the $\varepsilon > \varepsilon_0$ region. ν_0, in turn, depends strongly on $\mathcal{D}_{\Gamma x}$: $\nu_0 \sim \mathcal{D}_{\Gamma x}^2$. $\mathcal{D}_{\Gamma x}$ seems large enough and is of the order of 10^9 eV cm^{-1} [10]. In this case the assumption that the $\varepsilon > \varepsilon_0$ region is narrow is valid, and the quantitative results given here are plausible. Otherwise negative differential conductivity also appears during cyclotron resonance, but the results will be of a qualitative character.

According to our estimates the plasma frequency of the free-electron system at an impurity concentration of 10^{16} cm^{-3} and at temperatures near 77 K is considerably smaller than the wave frequency in the terahertz range. Therefore we believe that the operating temperature of the systems that we are investigating may be considerably higher than 4 K. In particular, it may be increased up to the liquid-nitrogen temperature.

One of the main conclusion of our investigations is that the radiation frequency can be smoothly varied within a certain, rather wide range. This can be achieved by H variation if condition (9) is fulfilled.

References

[1] McIntosh K A, Brown E R, Nichols K B, McMahon O B, Di Natale W F and Lyszczarz K B 1995 *Appl. Phys. Lett.* **67** 3844

[2] Igantov A A, Renk K F and Dodin E P 1993 *Phys. Rev. Lett.* **70** 1996

[3] Vorobjov L E, Donetzki D V, Kastalski A, Golub L E, Aleshkin V Ja, Orlov L K and Kuznetsov O A 1996 *Abtracts 2nd Russian Conf. on the Physics of Semiconductors* vol 1 p 164

[4] Vorobjov L E, Danilov S N, Donetzki D V, Kochegarov Yu V, Stafeev V I and Firsov D A 1996 *Abstracts 2nd Russian Conf. on the Physics of Semiconductors* vol 2 p 42

[5] Dzamukashvili G E, Kachlishvili Z S and Metreveli N K 1995 *Zh. Eksp. Teor. Fiz. Pis. Red.* **62** 220
[6] Levinshtein M E and Shur M S 1975 *Fiz. Tekh. Poluprov.* **9** 617–49
[7] Andronov A A and Dzamukashvili G E 1985 *Solid State Commun.* **55** 915
[8] Vosilius V V and Levinson I B 1967 *Zh. Eksp. Teor. Fiz.* **52** 1013
[9] Adachi S 1985 *J. Appl. Phys.* **53** R1
[10] Saxena A K and Gurumurthy K S 1982 *J. Phys. Chem. Solids* **43** 801